ANL-HEP-CP--86-94 03--8

DE87 001555

PARTICLE PRODUCTION IN e^+e^- ANNIHILATION AT 29 GeV

M. Derrick
Argonne National Laboratory
Argonne, IL 60439

Recent results on particle production in e^+e^- annihilation at 29 GeV are reviewed. The data were obtained using the High Resolution Spectrometer at PEP and correspond to an integrated luminosity of 300 pb^{-1}. The mean charged particle multiplicity in gluon jets from the three-jet events is found not to differ from that measured for quark jets. The production of the scalar meson S(975) and the tensor mesons $f^o(1270)$ and $K^*(1430)$ are observed and the rates are compared to the previously observed vector mesons, ρ and $K^*(890)$. Finally, some of the global properties of charged particle production are presented and compared with similar results from soft hadronic collisions.

INTRODUCTION

The characteristics of particle production in high energy reactions has been an important topic in physics for many years. Before the successful application of QCD to hard processes caused a switch of interest to studies of high q^2 reactions, a phenomenological picture of the nature of high energy hadronic reactions was developed as a result of experiments done at the ISR and with the 30" bubble chamber at Fermilab.[1] Since multihadron production in e^+e^- annihilation is thought to be particularly simple and is well represented by QCD-based fragmentation models[2], it is of interest to see to what extent the e^+e^- data and the hadronic data differ. Such comparisons may be revealing of how often, for example, the final state in soft hadronic collisions results from the superposition of

Invited paper given at the XVII Symposium on Multiparticle Dynamics, Seewinkle, Austria (June 1986).

DISCLAIMER

more than one parton-parton interaction.

A significant fraction of e^+e^- events at 29 GeV result from the $q\bar{q}g$ partonic state and so some information on gluon fragmentation can be obtained.

Finally, the recent data on scalar vector and tensor mesons is reviewed with with particular reference to the nature of the S(975) and δ(980) particles.

The results presented are based on data taken with the High Resolution Spectrometer (HRS) operated at the e^+e^- storage ring (PEP) at a cm energy of 29 GeV. The total data sample corresponds to an integrated luminosity of 300 pb^{-1} yielding ~ 116 K hadronic events.

EXPERIMENTAL DETAILS

The HRS is a solenoidal spectrometer[3] that measures charged particles and electromagnetic energy over 90% of the solid angle. The tracking system consists of a vertex chamber, a central drift chamber, and an outer drift chamber. The central drift chamber has 15 layers of cylindrical drift planes, eight of which have stereo wires (±60 mrad) in order to measure the position along the e^+e^- beam direction. The momentum of charged particle in the 1.62 T magnetic field is measured with a resolution of 3% at 14.5 GeV. The minimum momentum for detecting tracks with good efficiency is about 200 MeV/c. The 40-module barrel shower counter system provides electromagnetic calorimetry over 62% of the solid angle with energy resolution of $\sigma_E/E = 0.16\sqrt{E\ (GeV)}$.

The beam pipe and the inner wall of the central drift chamber are made of beryllium so as to minimize the conversion of photons into electron-positron pairs; the total material between the interaction point and the central drift chamber is less than 0.02 radiation lengths.

The multiplicity study[4] is based on a subsample of the data (185 pb^{-1}) and to ensure good tracking efficiency, the thrust axis of the event was selected to be within 30° of the equatorial plane of the

detector, and each track had to have an angle with respect to the e^+e^- beam direction of more than 24° and had to register in more than one-half of the drift chamber layers traversed. With these selections, the reconstruction efficiency to isolated tracks was greater than 99%. For a typical annihilation event, with several close neighboring tracks, the reconstruction efficiency was 80% or better. This data sample contains 29,649 events.

In addition to the inclusive data set, a sample of two-jet events was selected with sphericity less than 0.25 and an aplanarity less than 0.10. These cuts, which exclude the events with hard gluon radiation, gave a data sample of 24,553 collimated and planar events.

RESULTS

a. Gluon Jet Multiplicity

For the gluon jet measurements[5] and the resonance production study, the full data set was used.

A sample of three-jet events was selected using a jet-finding algorithm applied to the data with sphericity $S > 0.15$ and aplanarity $A < 0.1$. For each event, the values of the variables that maximized the longitudinal momentum along two or three axes were calculated. For two- (three) jet events, this is the thrust (triplicity) variable.

The ratio of triplicity to thrust was required to be greater than 1.05, and with this selection ~ 90% of the $q\bar{q}g$ partonic states were selected with a background from the two-jet $q\bar{q}$ states of ~ 15%. The corrected mean multiplicity of the individual jets as a function of their energy is shown in Fig. 1. Although jet 3

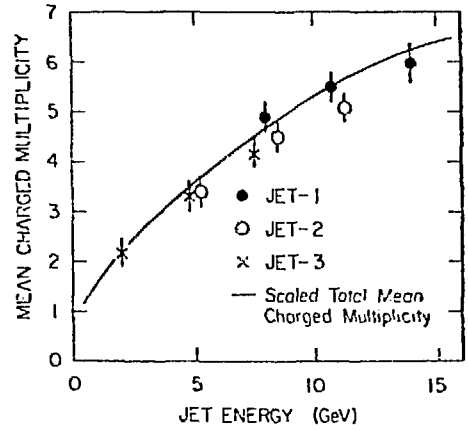

Fig. 1. Mean charged particle multiplicity as a function of jet energy.

is enriched in gluon fragmentation (~ 56% of the third jets originate from gluons), there is no difference between the mean multiplicity of any of the three jets. The line, which agrees with the data, shows the variation of the single jet multiplicity for all e^+e^- annihilation, plotted against $\sqrt{s}/2$. This is a somewhat surprising results since the 9/4 ratio of ggg to $gq\bar{q}$ coupling should result in gluon jets having about twice the quark multiplicity. A study of the symmetric three-jet events shows that the ratio $< n >_g / < n >_q = 1.25 \; ^{+\,0.17}_{-\,0.32} \pm 0.20$ for a jet energy of 9.7 GeV. A recent paper by Dzhaparidze[6] shows that this result can be reconciled with the 9/4 ratio expected at infinite energies when the large fraction of energy carried by the heavy quarks (c and b) and the low energy of the jets in the present experiment are taken into account.

b. Scalar, Vector, and Tensor Meson Production

The production of the vector mesons ρ^o and $K^*(890)$ has been measured by several e^+e^- collaborations.[7] We have recently extended these observations to the scalar S(975) and the tensor mesons $f^o(1270)$ and $K^{*o}(1430)$.[8]

Since no particle identification was used, all tracks were considered as pion and kaon candidates and were used to calculate the $\pi^+\pi^-$ and $K^\pm\pi^\mp$ invariant masses. The doubly charged $\pi^\pm\pi^\pm$ and $K^\pm\pi^\pm$ spectra were also generated. A reduction in the combinatorial background of the mass spectra was obtained by requiring that $|\cos\theta^*| < 0.65$, where θ^* is the decay angle in the rest frame of the two-particle system relative to the jet axis. The mass spectra, obtained for doubly-charged combinations, were subtracted from the corresponding neutral charge combination.

Figure 2(a) shows the subtracted $\pi^+\pi^-$ mass spectrum between 0.64 GeV and 1.62 GeV. These data were selected with $x > 0.2$, where x is the fractional momentum of the two-particle system ($x = p/p_{beam}$). Figure 2(b) shows the equivalent spectrum for the $K\pi$ combinations with mass between 0.8 GeV and 1.67 GeV and with $x > 0.2$. Peaks corresponding to the (S, ρ, f^o) and the two neutral K^*'s can be seen.

The production characteristics of the f^o, $K^{*o}(1430)$, and S mesons were extracted from these spectra by an overall fitting procedure. For example, the $\pi^+\pi^-$ mass spectrum of Fig. 2(a) was fit assuming contributions from the ρ, S, and f^o signals, as well as reflections from $K^{*o}(890)$ and $K^{*o}(1430)$.

The solid curves in Figs. 2(a) and 2(b), which show the final fits, have χ^2/DOF of 32/29 and 35/28, respectively. An increase of 20 (9) in the χ^2 resulted when the fit to the $\pi\pi$ ($K\pi$) spectrum was repeated without the f^o ($K^*(1430)$) resonance term. In the $\pi\pi$ spectrum, the χ^2 was increased by 14 when the S mesons was ignored in the fit. In the fits, the masses and widths of the resonances were fixed to their established values. For the narrow S signal, the detector mass resolution of 15 MeV was added to the width in quadrature. The dashed curves in Fig. 2 show the contribution from the smooth background and the reflection from the wrong mass assignments. The area between the dotted and dashed curve represents the reflection of the $K^*(1430)$ or f^o peaks.

In Fig. 2(b) the contributions from $K^*(890)$ and $K^*(1430)$, whose masses and widths were again fixed to the known values, are evident.

The solid curve in the insert of Fig. 2(a) shows the result of the fit in the S meson region. After correcting for the detector resolution, we find a mass of 978 $\pm$ 9 MeV, and a full width of 29 $\pm$ 13 MeV for the S peak, in agreement with the world average values.

Differential cross sections were measured by repeating the simultaneous fits to the $\pi\pi$ and $K\pi$ mass spectra in different x intervals and are shown in Fig. 3. The errors bars are dominated by the systematics. The acceptances, which were calculated by Monte Carlo techniques, were typically $\sim$ 50%. The correction for the decay angle (θ^*) cut was made assuming isotropic decay in the c.m. frame. The established branching ratios were used to include contribution from other decay channels.

We have compared our results on the tensor mesons with the predictions of the Webber cluster model.[2] In this approach, the

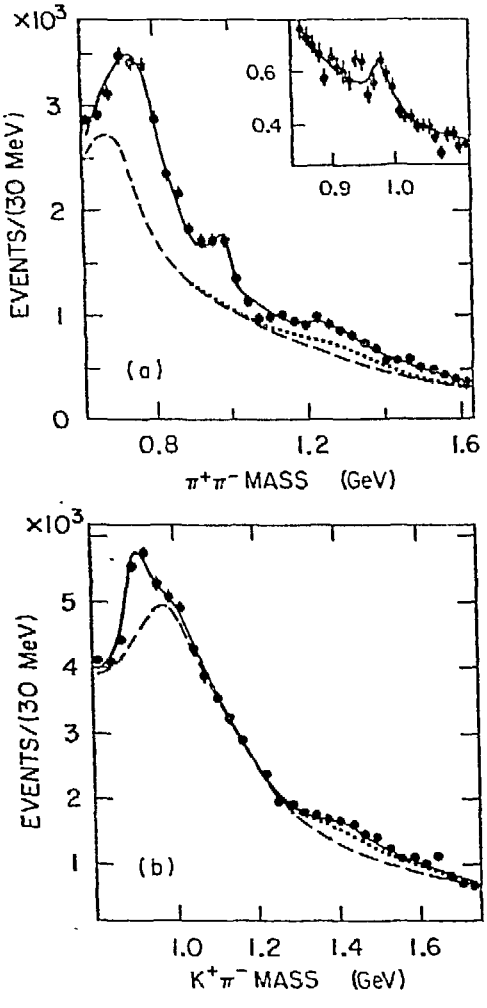

Fig. 2. $\pi^+\pi^-$ and $K^+\pi^-$ mass spectra after subtracting the doubly-charged combinations.

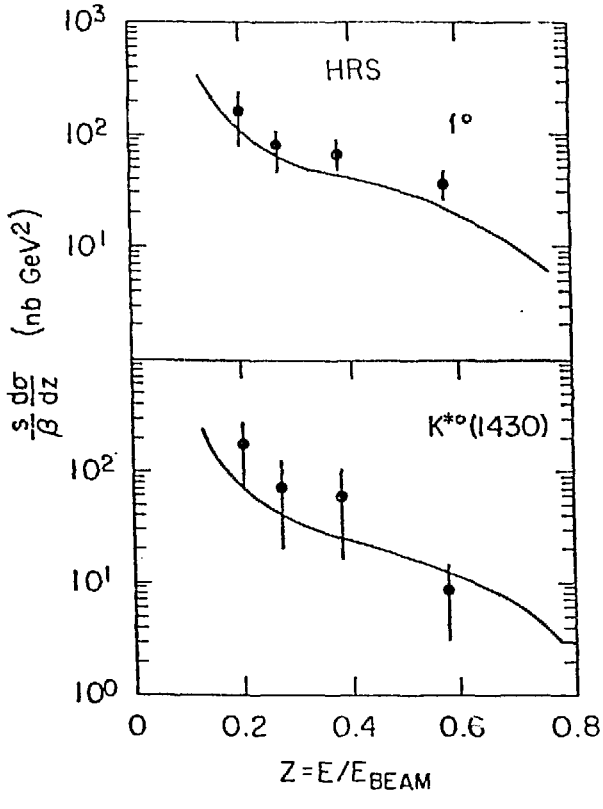

Fig. 3. Scaling cross section for the production of the tensor mesons.

production rates are determined by the phase space available in the decay of clusters, and so the tensor mesons should be suppressed relative to the lighter mesons. The predicted scaling cross sections for f^o and $K^*(1430)$ are shown by the lines in Fig. 3; the agreement with the data is good. The results have been extrapolated to the low x region using this shape and give total multiplicities of 0.14 ± 0.04 f^o and 0.12 ± 0.06 $K^*(1430)$ per hadronic event, as compared to 0.95 ± 0.09 ρ^o and 0.63 ± 0.10 $K^{*o}(890)$ per hadronic event previously reported.[7] We note that the S meson multiplicity of 0.05 ± 0.02 for $x > 0.1$ is lower than those of the heavior f^o and $K^*(1430)$ mesons.

Since the 0^{++} states are not included in the present version of the Webber Monte Carlo, the measured S(975) meson multiplicity was compared with the prediction of this model for the production of the $\eta'(985)$, coming entirely from the $s\bar{s}$ clusters. The model gives 0.033 $\pm$ 0.001 η' per event for $x > 0.1$, in good agreement with our measured value. This result on its own does not discriminate between the S being a four-quark $K\bar{K}$ bound state or a member of the scalar octet with ideal mixing. To resolve these two options, it is necessary to measure the production of the $\delta(980)$, the isovector partner of the S. If both the S and δ are members of the scalar octet, then the δ^o should consist primarily of non-strange quarks and so be produced with ~ 3 times the rate of the S^o. If they are both $K\bar{K}$ bound states, then the S^o and δ^o production rates should be equal. The detection of the δ is more difficult since it decays to $\eta\pi$ and no results are yet available.

c. Multiplicity Distributions

I now present some aspects of the multiplicity distributions.[4] If the events are divided into two jets by a plane perpendicular to the thrust axis for the single jets, charged particle multiplicity distribution shown as the histogram in Fig. 4(a) is obtained. This distribution has a mean value of $< n > = 6.26 \pm 0.02 \pm 0.15$, a dispersion, $D_2 = (< n^2 > - < n >^2)^{1/2} = 2.45 \pm 0.02 \pm 0.12$ and an f_2 moment, $f_2 = < n(n-1) > - < n >^2 = -0.26 \pm 0.03 \pm 0.13$: the first error is statistical and the second systematic. The full line connects values of a Poisson distribution $P(n) = \frac{< n >^n}{n!} e^{-< n >}$ calculated with $< n > = 6.26$. It agrees well with the data, as expected from the value of the f_2 moment which should be zero for such a distribution. The dashed line shows a Poisson in n/2, which might be more appropriate if pairs of opposite charged particles were emitted.[9] This curve clearly does not agree with the data histogram.

The multiplicity distribution for the total event is shown in Fig. 4(b). Again, the line connects points on a Poisson distribution with the same mean value. This data has $< N > = 2< n >$ by definition

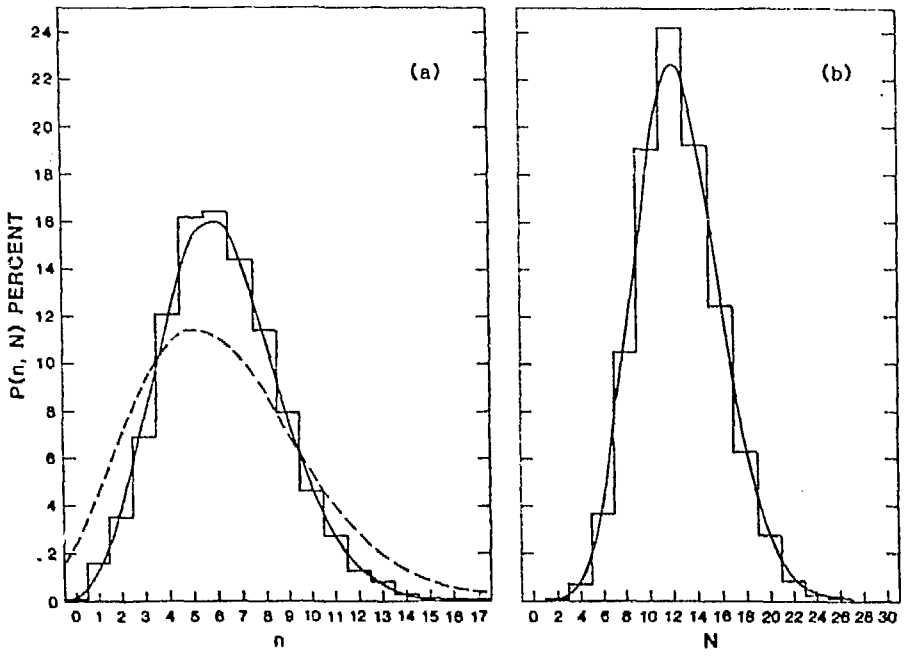

Fig. 4. The histograms show the charged particle multiplicity distributions for two-jet events: (a) single jet, (b) whole event. The full lines connect points on a Poisson distribution with the same mean values. The dashed line in (a) shows a Poisson distribution of pairs.

and a dispersion $D_2 = 3.48 \pm 0.02 \pm 0.17$ which is $\sqrt{2}$ times larger than $D_2 = 2.45 \pm 0.02 \pm 0.12$ measured for the single jets.

The variation of $\langle n \rangle_B$ with n_F, shown in Fig. 5, is flat. The slight rise at low n_F values comes from the cut at $m = 5$ (m is the observed number of charged particles per event) that is used to exclude the low multiplicity tau pair events. The line shows the result of a simple calculation using the measured $\langle N \rangle$ values for (u,d,s) c and b quarks,[10] as well as the effect of the cut at $m = 5$. A fit to the data of Fig. 5 with $n_F \geq 6$ to $\langle n_B \rangle = a + b\, n_F$ gives $b = -0.001 \pm 0.015$.

The Poisson multiplicity distribution for single jets, the $\sqrt{2}$ difference between the widths of the single jet and complete multiplicity distributions, and the lack of an F:B correlation support the idea of independent jet fragmentation to individual hadrons. This can be further investigated by looking at the F:B split for fixed total

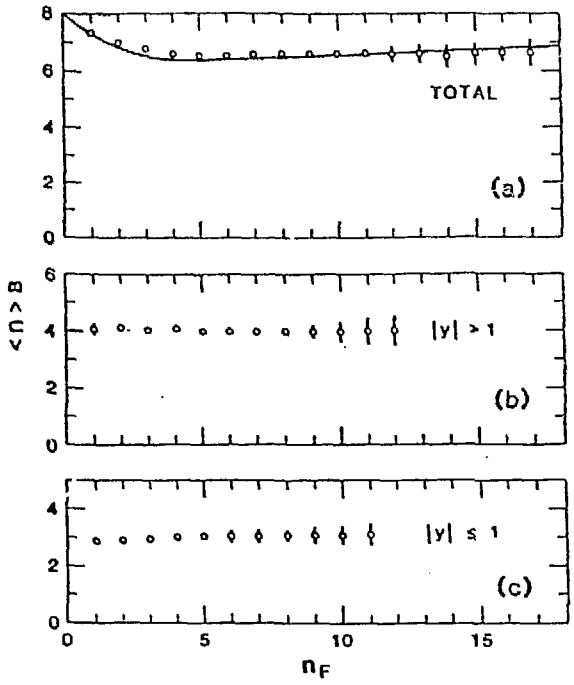

Fig. 5. Forward:backward multiplicity correlations for (a) full rapidity span, (b) tracks with $|Y| \leq 1.0$ removed, (c) tracks in the region $|Y| \leq 1.0$. The errors shown are dominated by the systematic uncertainties. The line shows the results of the simple calculation described in the text.

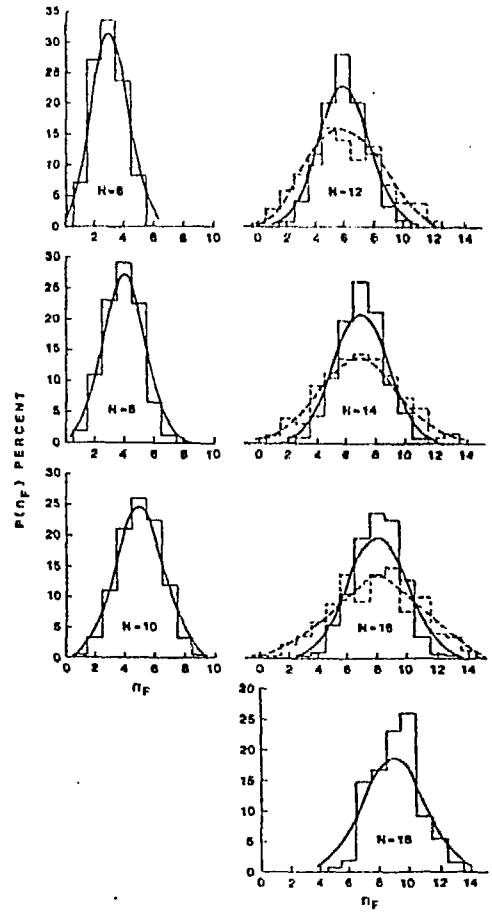

Fig. 6. The full histogram show the forward:backward charged particle multiplicity splits for fixed total multiplicity (N) for N = 6 to N = 18. The full lines connect points on a binomial distribution.

multiplicity N. These data for N = 6 and N = 18 are shown as the histogram of Fig. 6. The lines, which connect the points on binomial distributions,

$$P_n(n_F) = \frac{N!}{n_B!\ n_F!} \left(\frac{1}{2}\right)^{n_B} \left(\frac{1}{2}\right)^{n_F} .$$

represent the histograms well.

The dashed histograms in Fig. 6 for N = 12, 14, 16 show the results of the UA5 experiment.[11] These distributions are clearly wider than the e^+e^- data, and are well represented by the dashed lines, which correspond to binomial distribution of pairs. These hadronic distributions have been interpreted as due to charge conservation,[9] or to the dominance of the reactions by charge neutral clusters.[12] Since charge conservation also holds for e^+e^- annihilation, it seems unlikely that the differences in the F:B distributions at fixed N for e^+e^- and hadronic collisions arises from these effects.

The e^+e^- data given here support the simplest picture of independent emission of single charged particles from the uncorrelated fragmentation of the two jets of the event. However, as we have discussed, the e^+e^- final states, in common with the hadronic reactions, include many resonances such as ρ^o, $K^*(890)$, f^o, $K^*(1420)$, etc. In addition, 40% of the e^+e^- events have two mesons or baryons containing the heavy quarks, c and b. These heavy quark states decay to several π and K mesons.

The charged particle multiplicity distribution for the two-jet events expressed in KNO form using the scaling variable $Z = n/\langle n \rangle$ is shown in Fig. 7, where $\psi(Z)$ is defined as $\psi(Z) = \langle n \rangle \frac{\sigma_n}{\Sigma\sigma_n}$.

The figure[13] shows both the total sample and the distributions for particles contained in selected rapidity ranges from $|Y| < 0.1$ to $|Y| < 2.5$, corresponding to Y spans from 0.2 to 5.0 units. Each successive data set has been displaced lower by a factor of ten for clarity. The uncut events are always even prongs so the normalization differs by a factor of two from that of the data with a rapidity selection. This distribution is quite narrow, not much exceeding $Z \sim 2$. The distributions clearly widen as the rapidity span is restricted, and for $Y \lesssim 1$ events with Z values of 4 to 5 are seen.

The multiplicity distributions for the data in the outer regions of the rapidity span has also been studied. In all cases, the distribution is narrow, even when the Y range selected is small.

The data of Fig. 7 have been fitted to the negative binomial expression

$$P(n, \langle n\rangle, k) = \frac{k(k+1)\ \ldots\ (k+n-1)}{n!} \times \left(\frac{\langle n\rangle/k}{1+\langle n\rangle/k}\right)^{n} \left(1+\frac{\langle n\rangle}{k}\right)^{-k}$$

In this parameterization, the shape of the distribution is determined by the parameter k and the position of the maximum by $\langle n \rangle$. The variable k is related to the mean multiplicity $\langle n \rangle$ and the dispersion D by

$$\frac{D^2}{\langle n \rangle^2} = \frac{1}{\langle n \rangle} + \frac{1}{k} \quad .$$

The values of $\langle n \rangle$ and k resulting from the fit the NB are given in Table I. The k value falls rapidly as the Y limit is restricted but levels off for the central rapidity range with a k value of ~ 5.

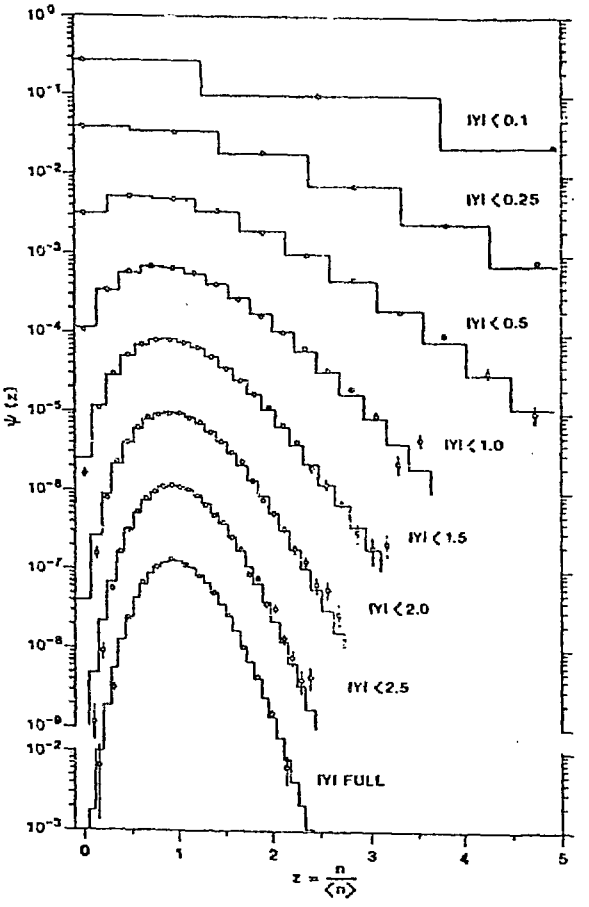

Fig. 7. Multiplicity distributions for two-jet events of e^+e^- annihilation at 29 GeV as a function of the rapidity span selection. The histograms show the best fit to the negative binomial. Each of the selected distributions has been shifted down by a factor of ten relative to the $|Y| < 0.1$ data. The ordinate scale for the data set with no rapidity selection is shown separately.

Table I
Fits to the Negative Binomial

Rapidity Range $\|Y\|$	Two-Jet Data		Inclusive Data	
	k	$\langle n \rangle$	k	$\langle n \rangle$
< 2.5	57.18 ± 2.62	10.83 ± 0.02	38.50 ± 0.86	11.38 ± 0.01
< 2.0	26.18 ± 0.66	8.97 ± 0.02	17.45 ± 0.36	9.70 ± 0.02
< 1.5	15.95 ± 0.41	6.65 ± 0.02	10.57 ± 0.15	7.39 ± 0.01
< 1.0	10.56 ± 0.27	4.27 ± 0.01	6.99 ± 0.05	4.82 ± 0.02
< 0.5	7.32 ± 0.30	2.12 ± 0.01	5.53 ± 0.19	2.35 ± 0.01
< 0.25	6.14 ± 0.20	1.06 ± 0.01		
< 0.1	4.85 ± 0.50	0.403 ± 0.005	4.42 ± 0.29	0.427 ± 0.002

This variation of k with Y differs qualitatively from the observation of the UA5 group[14] who studied $\bar{p}p$ interactions at $\sqrt{s}$ = 546 GeV and found a continuous broadening of the multiplicity distributions as the pseudorapidity ranges was narrowed: no tendency to a limiting shape was seen. However, the result data of the NA22 collaboration[15] studying $\pi^+ p$ and pp interactions at $\sqrt{s}$ = 22 GeV also show a flattening in the k:ΔY plot for small ΔY values.

DISCUSSION

The full richness of the phenomena in e^+e^- annihilation to hadrons has not yet been explored. As higher precision data becomes available, new details are seen. A complete phenomenological description of quark fragmentation can only come from studies of deep inelastic scattering and e^+e^- annihilation and is an essential input to QCD models that are being developed to describe high p_T hadronic interactions.[16]

A comparison of e^+e^- data and results from soft hadronic collisions can be revealing of the basic processes responsible for the latter. This is important as, at present, there is no theoretically

well-founded description of soft processes. The comparisons of the multiplicity distributions presented here suggest that the neutral clusters that provide a useful description of many phenomena seen in the hadronic data cannot be identified with resonances. One obvious possibility is that the effects in the hadronic data are a manifestation of multiple parton (gluon) interactions with a given hadronic collision, so that the hadronic final states are a superposition of different incoherent reactions. This observation is in agreement with the assumptions underlying several models of hadronic collisions. For example, the dual parton model, which is based on the marriage of Regge ideas and the quark structure of hadrons, considers pp interactions to go via the exchange of two chains.

ACKNOWLEDGMENTS

This program of research has been carried out by physicists from Argonne and the Universities of Indiana, Michigan, and Purdue. S. Abachi, P. Kooijman, M. Nappi, and K. Sugano have been particularly associated with the prsent work. This research was supported in part by the U.S. Department of Energy, under Contracts W-31-109-ENG-38, DE-AC02-76ER01112, DE-AC03-76SF00098, DE-AC02-76ER01428, and DE-AC02-84ER40125.

REFERENCES

1. Whitmore, J., Phys. Rep. 10C, 273 (1974), 27C, 187 (1976); Foa, L., ibid., 22, 1 (1975); Giacomelli, G. and Jacob, M., ibid. 55, 1 (1979).
2. Andersson, B. et al., Phys. Rep. 97, 32 (1983); Gottschalk, T., Nucl. Phys. B214, 201 (1983); Webber, B., ibid. B238, 492 (1984).
3. Bender, D. et al., Phys. Rev. D30, 515 (1984), D31, 1 (1985).
4. A detailed discussion is given in: Derrick, M. et al., ANL-HEP-PR-86-03, Phys. Rev. D (to be published).
5. Derrick, M. et al., Phys. Lett. 165B, 449 (1985). The present paper updates these results with the full data sample.

6. Dzhaparidze, D. Sh., "Comparison of Hadron Multiplicities in Gluon and Quark Jets," Serpukhov preprint (1986).
7. Derrick, M. et al., Phys. Lett. 158B, 519 (1985) and references therein.
8. Abachi, S. et al., ANL-HEP-CP-86-70, Phys. Rev. Lett. (to be published).
9. Chou, T. T. and Yang, C. N., Phys. Lett. 135B, 175 (1985), 167B, 453 (1986); Phys. Rev. Lett. 55, 1359 (1985).
10. Sakuda, M. et al., Phys. Lett. 152B, 399 (1985); Kesten, P. et al. ibid. 161B, 412 (1985).
11. Alpgard, P. et al., Phys. Lett. 123B, 361 (1983); Asman, B., Thesis, Stockholm (1985) unpublished.
12. Cai Xu et al., Phys. Rev. D33, 1287 (1986).
13. Derrick, M. et al., Phys. Lett. 168B, 299 (1986).
14. Alner, G. J. et al., Phys. Lett. 160B, 193 (1985).
15. Adamus, M. et al., "Rapidity Dependence of Negative and All-Charged Multiplicities in Non-Diffractive π^+p and pp Collisions at 250 GeV/c", HEN-273 (1986).
16. Derrick, M. and Gottschalk, T., Proc. of the 1984 Summer Study on the Design and Utilization of the Superconducting Super Collider, p. 49 (Snowmass, CO).

DISCUSSION

R. Szwed - Warsaw

The usual, well understood and proven way of searching for clusters is a correlation study. You claim that you do not see any clusters, so I would like to see two particle correlations functions for a fixed multiplicities and check myself if they are flat.

M. Derrick

There are, of course, strong two particle correlations in rapidity, qualitatively quite similar to what we have known in hadron physics for a long time. The point I am making is that the global multiplicity variables in e^+e^- do not show evidence for clusters, whereas in the hadron physics they do.

Bialas - Krakow

What is the expected average number of charged particles per cluster in your data if you identify clusters with resonances?

M. Derrick

Although such estimates are notoriously unreliable, from the known resonance production, including heavy flavor mesons, one can estimate an average of 1.6 charged particles per cluster.

Wroblewski - Warsaw

You have shown that there are many resonances in e^+e^- so particles are not produced simply. On the other hand, from the negative binomial machinery you get the cluster multiplicity equal to one. I think that it proves that the answer that one gets from the negative binominal does not have any clear physics interpretation.

M. Derrick

That is certainly one possibility.

A. Capella - ORSAY

An important difference between e^+e^- and h h is the following: in a 2-jet e^+e^-, the ends of the string are fixed in rapidity whereas in hh they are distributed according to structure functions. If this effect is taken into account the average multiplicity per cluster goes down to 1.3 or 1.4 (see A. Capella in Proc. $\bar{p}p$ meeting, St. Vincent, 1985). What is the value of $D^2/< n >$ for $|Y| < 1$?

M. Derrick

The D and $< n >$ values as a function of rapidity span are given in Phys. Lett. 168B, 299 (1986). For $|Y| < 1$ the ratio $D^2/< n >$ is about 6.

R. Sosnowski - Warsaw

Gluon jets are expected to fragment with a softer spectrum of secondaries than is the case for quark jets. Some e^+e^- and hadronic data support this expectation. From this it is followed that the average multiplicity of gluon fragments has to be higher than that of quark fragments, contrary to your data. Does your data show that gluon rich jets have softer fragments than quark rich jets?

M. Derrick

We have not yet done this. There is, however, data from the MARK II giving the ratio of the gluon and quark fragmentation functions that shows the effect your mention. However, the lowest x point, where all the multiplicity is concentrated, shows no enhancement of gluon over quark.

C. Heusch - Santa Cruz

Would you care to comment on the difference between the TASSO and the HRS multiplicity distributions?

M. Derrick

The low multiplicities were taken from the Monte Carlo for TASSO, whereas the HRS group used the independent fragmentation of the two jets to measure the low multiplicity cross sections. The restriction of the HRS events to the central region of the spectrometer also means that the higher multiplicities are easier to measure.

A. Eskreys - Krakow

I agree that prong selection in TASSO data was not as elaborate as was done by HRS collaboration and that may be the reason for differences in multiplicity distributions between HRS and TASSO.

A. Eskreys - Krakow

If the total multiplicity distribution of the HRS in KNO form is clearly narrower than that from TASSO, why do the single jet KNO functions agree quite well?

M. Derrick

I think that this comes about because the higher multiplicity events tend to be more isotropic. For example, a single jet with $Z = 2$ (13 prongs) is easier to measure if the multiplicity in the opposite jet is small. A total event with $Z = 2$ has 26 prongs many of which can overlap each other.

Chao Wei-qin - Beijing

Our analysis of the multiplicity distributions in different Y windows (Berlin preprint FUB HEP 86/3) shows that the effect is merely statistical and gives no dynamical insights.

M. Derrick

To obtain a good representation of the HRS data (Fig. 7), you have to assume a F:B distribution as a binominal of pairs contrary to the results shown in Fig. 6.

Chao Wei-qin

The binomial F:B correlation follows from the Poisson observed for each jet. The latter may be an accident coming from folding a sub-Poissonian cluster distribution with a cluster decay.

M. Derrick

Yes indeed, but don't tell Frank Yang.